THE JOURNAL OF BIOLOGICAL CHEMISTRY VOL. 286, NO. 30, pp. 26873–26887, July 29, 2011

Silencing Suppressor of Cytokine Signaling-1 (SOCS1) in Macrophages Improves *Mycobacterium tuberculosis* Control in an Interferon-γ (IFN-γ)-dependent Manner*[S]

Received for publication, March 9, 2011, and in revised form, May 6, 2011 Published, JBC Papers in Press, May 27, 2011, DOI 10.1074/jbc.M111.238287

Berit Carow[‡1], Xiang qun Ye[‡1], Dolores Gavier-Widén[§], Sabin Bhuju[¶], Wulf Oehlmann[¶], Mahavir Singh[¶], Markus Sköld[‡], Lech Ignatowicz[‡], Akihiko Yoshimura[‖], Hans Wigzell[‡], and Martin E. Rottenberg[‡2]

From the [‡]Department of Microbiology, Tumor and Cell Biology, Karolinska Institutet, Stockholm 17177, Sweden, the [§]Department of Biomedical Sciences and Veterinary Public Health, Swedish University of Agricultural Sciences, 75007 Uppsala, Sweden, [¶]Lionex GmbH, 38126 Braunschweig, Germany, and the [‖]Department of Microbiology and Immunology, Keio University School of Medicine, 160-8582 Tokyo, Japan

Protection against infection with *Mycobacterium tuberculosis* demands IFN-γ. SOCS1 has been shown to inhibit responses to IFN-γ and might thereby play a central role in the outcome of infection. We found that *M. tuberculosis* is a highly efficient stimulator of SOCS1 expression in murine and human macrophages and in tissues from infected mice. Surprisingly, SOCS1 reduced responses to IL-12, resulting in an impaired IFN-γ secretion by macrophages that in turn accounted for a deteriorated intracellular mycobacterial control. Despite SOCS1 expression, mycobacteria-infected macrophages responded to exogenously added IFN-γ. SOCS1 attenuated the expression of the majority of genes modulated by *M. tuberculosis* infection of macrophages. Using a conditional knockdown strategy in mice, we found that SOCS1 expression by macrophages hampered *M. tuberculosis* clearance early after infection *in vivo* in an IFN-γ-dependent manner. On the other hand, at later time points, SOCS1 expression by non-macrophage cells protected the host from infection-induced detrimental inflammation.

Tuberculosis, an infectious disease caused by *Mycobacterium tuberculosis*, remains a leading public health problem worldwide. The global incidence of tuberculosis is rising, with 8.8 million new cases and 2 million deaths each year (1).

In most cases, the human immune system is able to control bacterial replication and prevent development of active disease. The rate of progression from colonization to disease is low, and ~90% of infected individuals never develop clinical disease. However, *M. tuberculosis* is able to prevent the host immune response from totally eliminating the microorganism. Thus, the host becomes chronically infected.

A host counters mycobacterial infections primarily via Th1 immune responses involving cellular effector mechanisms, such as macrophage activation. IFN-γ is known to be an important mediator of macrophage activation and intracellular control of pathogens, including mycobacteria (2). Disseminated *M. tuberculosis* is observed in *IFN-γ*-deficient mice (3, 4). Individuals with defects in genes involved in the secretion or signaling of IFN-γ are even susceptible to weakly virulent mycobacteria (5). However, the expression of selected IFN-γ-inducible genes is paradoxically decreased in macrophages infected with mycobacteria (6–8). It remains unclear how mycobacteria-induced signaling contributes to macrophage dysfunction.

Immune and inflammatory systems are controlled by multiple cytokines, including interleukins and interferons. Many cytokines exert their biological function through Janus kinases (JAK) and signal transducers and activators of transcription (STAT). SOCS (suppressor of cytokine signaling) is a family of eight intracellular proteins. SOCS proteins function in a negative feedback loop to inhibit cytokine signaling by binding to either JAK or the cytokine receptor, either inhibiting JAK activity directly or targeting the receptor complex for ubiquitination and subsequent proteasome-mediated degradation (9).

SOCS1, one of the better described of the family members, has been reported to inhibit STAT1-mediated responses (10, 11). The vital importance of SOCS1 is stressed by the fact that *SOCS1*$^{-/-}$ mice die within 3 weeks after birth with severe lymphopenia, necrosis of the liver, and mononuclear infiltration of several organs (12, 13). The neonatal defects exhibited by *SOCS1*$^{-/-}$ mice appear to be due to increased production of IFN-γ by T and NKT cells and uncontrolled IFN-γ signaling in myeloid cells (12–14). Accordingly, T cell activation and differentiation is also regulated by SOCS1 (15, 16). Besides regulating IFN-γ signaling, SOCS1 is crucial in attenuating STAT1-mediated IFN-α/β signaling (17) and has also been shown to attenuate IL-12 (18), IL-4 (19), and other γ_c-dependent cytokine (20) signaling in myeloid and lymphoid cells.

SOCS1 is induced during infection of human macrophages with *Mycobacterium avium* (21) and in J774 cells infected with BCG[3] (22). Knockdown of *SOCS1* with shRNA has been recently shown to improve mycobacterial clearance in peripheral blood mononuclear cells (23). Given the indicated role of IFN-γ in the control of mycobacterial infections, we hypothesized that SOCS1 could play a central role by fine tuning the

* This work was supported by European Community Grant 200732 HOMITB, the Karolinska Institutet, and the Swedish Research Council.
[S] The on-line version of this article (available at http://www.jbc.org) contains supplemental Experimental Procedures, Table S1 and Figs. S1–S4.
[1] Both authors contributed equally to this work.
[2] To whom correspondence should be addressed. Fax: 468-304276; E-mail: Martin.Rottenberg@ki.se.

[3] The abbreviations used are: BCG, bacille Calmette-Guerin; BMM, bone marrow-derived macrophage(s); BMDC, bone marrow-derived dendritic cell(s); MOI, multiplicity of infection.

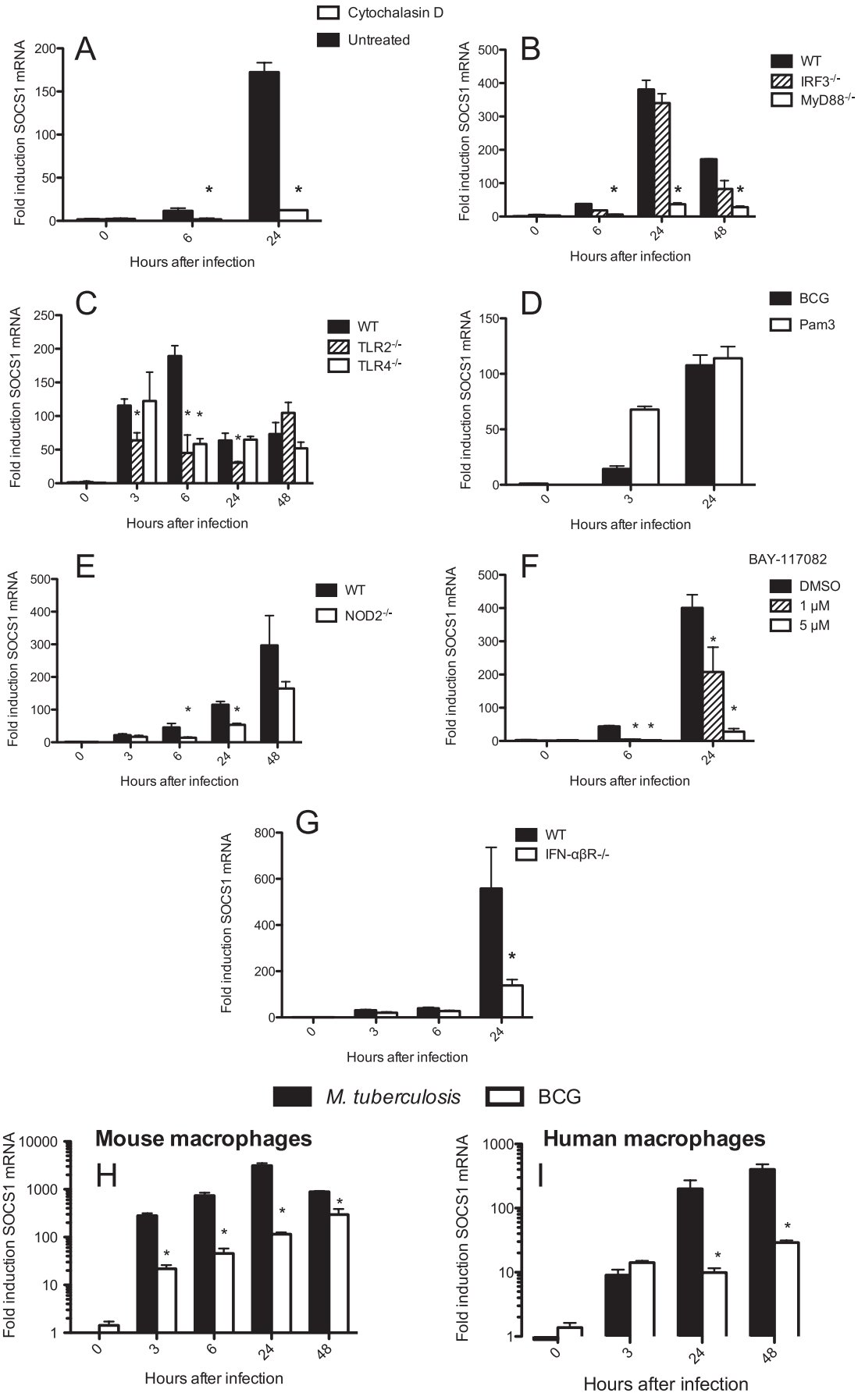
A
Cytochalasin D
Untreated
Fold induction SOCS1 mRNA
Hours after infection
B
WT
IRF3-/-
MyD88-/-
C
TLR2-/-
TLR4-/-
D
BCG
Pam3
E
NOD2-/-
F
BAY-117082
DMSO
1 μM
5 μM
G
IFN-αβR-/-
M. tuberculosis
BCG
Mouse macrophages
H
Human macrophages
I

balance between control of infection and generation of pathology during *M. tuberculosis* infection.

We studied the regulation and role of SOCS1 during mycobacterial infection of human and mouse macrophages as well as during infection *in vivo*. Infection efficiently stimulated SOCS1 expression in macrophages. Surprisingly, SOCS1 expression by macrophages regulated IL-12 rather than IFN-γ responses, resulting in diminished IFN-γ secretion and a less efficient bacterial control *in vitro* and early after infection of mice *in vivo*. Later after infection *in vivo*, SOCS1 expression by non-macrophage cells hampered a severe infection-induced inflammation.

EXPERIMENTAL PROCEDURES

Ethics Statement—All animal experiments were conducted in accordance with the guidelines of Karolinska Institutet and were approved by Stockholm's District Ethical Committee of Animal Research, permit numbers 302/10 and 415/08.

Mice—Mutant mouse strains with genomic deficiency in *SOCS1* (24), *MyD88* (25), *IRF3* (26), *TLR2* (27), *TLR4* (28), *NOD2* (29), *IFN-γ* (4), *IFN-γR* (30), *IFN-α/βR* (31), and *RAG1* (32) were generated by homologous recombination in embryonic stem cells. Animals were bred and kept under specific pathogen-free conditions. All mice were backcrossed to C57Bl/6 genetic background that was used as a control.

$RAG1^{-/-}/SOCS1^{-/-}$ mice were obtained by crossing $RAG1^{-/-}$ and $SOCS1^{-/+}$ mice (33). Similarly, $IFN\text{-}\gamma^{-/-}/SOCS1^{-/-}$ mice were generated by crossing of $IFN\text{-}\gamma^{-/-}$ and $SOCS1^{+/-}$ mice.

Tissue-specific *SOCS1*-deficient mice were generated using the cre/loxP system by breeding $SOCS1^{fl/fl}$ mice, which carry a *SOCS1* allele flanked by loxP sites (34), with mice expressing cre under the endogenous lysozyme M promoter (*LysM-cre*) (35), resulting in mice in which floxed *SOCS1* was deleted in myeloid cells. $SOCS1^{fl/fl}$ mice were generated on a C57BL/6 genetic background, whereas all other mice were 5th to 10th generation backcrosses to C57BL/6. $SOCS1^{fl/fl}$ littermates were used as controls in our experiments. The deletion of the *SOCS1* gene in macrophages but not in T cells from $SOCS1^{fl/fl}$ *LysM cre* mice was confirmed by PCR analysis (data not shown).

Generation of Mouse Bone Marrow-derived Macrophages and Dendritic Cells—Mouse bone marrow-derived macrophages (BMM) and dendritic cells (BMDC) were differentiated as described previously (36).

Generation of Human Monocyte-derived Macrophages—$CD14^+$ cells were isolated from peripheral blood from healthy donors by Ficoll-Hypaque, selected with anti-CD14 MACS beads (Miltenyi Biotech, Auburn, CA), and cultured in presence of GM-CSF as described (37).

Infection and Infectivity Assay—BCG Montreal and *M. tuberculosis* Harlingen and H37Rv were grown in Middlebrook 7H9 (Difco) supplemented with albumin, dextrose, catalase, and, for BCG cultures, 50 μg/ml hygromycin (Sigma).

BMM and BMDC were infected at the indicated MOI, and after 2 h, cells were washed twice with PBS to remove extracellular bacteria. Mice were infected intravenously with 1×10^6 BCG bacteria.

M. tuberculosis Harlingen strain was inoculated by the aerosol route using a nose-only exposure unit (Intox Products, Albuquerque, NM) as described previously (38). A 15-ml suspension of 0.5×10^6 *M. tuberculosis* was loaded into a nebulizer, and animals were exposed to the bacterial aerosol for 20 min. Bacteria were quantified on Middlebrook 7H11 agar containing a 10% enrichment of oleic acid, albumin, dextrose, catalase, 5 μg/ml amphotericin B, and 8 μg/ml polymyxin B grown for 3 weeks at 37 °C.

Real-time PCR—Transcripts were quantified by real-time PCR as described previously (39). The primer sequences used are shown in the supplemental Experimental Procedures.

Hprt was used as a control gene to calculate the ΔC_t values for individual samples. The relative amount of cytokine/*Hprt* transcripts was calculated using the $2^{-(\Delta\Delta C_t)}$ method as described. These values were then used to calculate the relative expression of cytokine mRNA in uninfected and infected cells and tissues.

Histopathological Analysis—Formalin-fixed samples of left lungs of mice experimentally inoculated with *M. tuberculosis* were blocked on paraffin. From each lung sample, four sections were obtained, one longitudinal along the long axis of the lobe and three across/transversal of the remaining piece of lung.

The blocks were processed, and sections were stained with hematoxylin-eosin. All sections were interpreted by the same pathologist and scored semiquantitatively, blinded to the variables of the experiment. The following features were scored: 1) lung area occupied with granulomas (percentage of the total area of the section); 2) lung area free of lesions or area of healthy lung (percentage of the total area of the section); 3) abundance of lymphocytes within the tuberculous lesions, ranging from 0 (not observed) to 4 (very large aggregates, often forming nodules); 4) abundance of lymphocytes in perivascular cuffs, ranging from 0 (not observed) to 4 (very thick lymphocytic cuffs); and 5) extension of necrosis, raging from 0 (no necrosis observed) to 4 (extensive necrosis and necrotic centers with mineralization).

Western Blotting—Uninfected and BCG or *M. tuberculosis*-infected BMM were lysed and separated on 10% separating, 5% stacking SDS-polyacrylamide gels as described (15). Samples were then transferred onto nitrocellulose membranes (Bio-Rad) by electroblotting at 100 V, 250 mA for 80 min. Immunostaining was performed using polyclonal rabbit anti-phosphorylated (Tyr^{701}) STAT1, total STAT1, or anti-ac-

FIGURE 1. **The expression of *SOCS1* mRNA in BCG-infected macrophages requires phagocytosis and the presence of innate TLR, NOD2, and IFN-α/β receptors.** Mouse BMM (*A–H*) or monocyte-derived human macrophages (*I*) were infected with BCG (*A–I*) or *M. tuberculosis* (*H* and *I*). BMM were treated or not with 5 μM cytochalasin D (*A*) or with the indicated concentrations of BAY-117082 (*F*) 1 h before BCG (*A–I*) or *M. tuberculosis* (*H* and *I*) infection. Total RNA was isolated from $IRF3^{-/-}$ (*B*), $MyD88^{-/-}$ (*B*), $TLR2^{-/-}$ (*C*), $TLR4^{-/-}$ (*C*), $NOD2^{-/-}$ (*E*), $IFN\text{-}\alpha/\beta R^{-/-}$ (*G*), and WT BMM (*A–H*) as well as from human macrophages (*I*) at the indicated times after infection with BCG. A MOI of 5:1 was used all over. Total RNA was also isolated after incubation of uninfected WT BMM with 1 μg/ml Pam3 (*D*). The accumulation of SOCS1 (*A–I*) and *Hprt* mRNA was measured by real time PCR. Duplicate determinations SOCS1 and *Hprt* mRNA were measured in triplicate samples for each group and time point. The mean -fold induction ± S.E. (*error bars*) is depicted. *, differences with WT (*B*, *C*, *E*, and *G*) or untreated (*A* and *F*) BMM are significant ($p < 0.05$, Student's *t* test). Differences with *M. tuberculosis*-infected mouse (*H*) or human (*I*) macrophages are significant ($p < 0.05$, Student's *t* test).

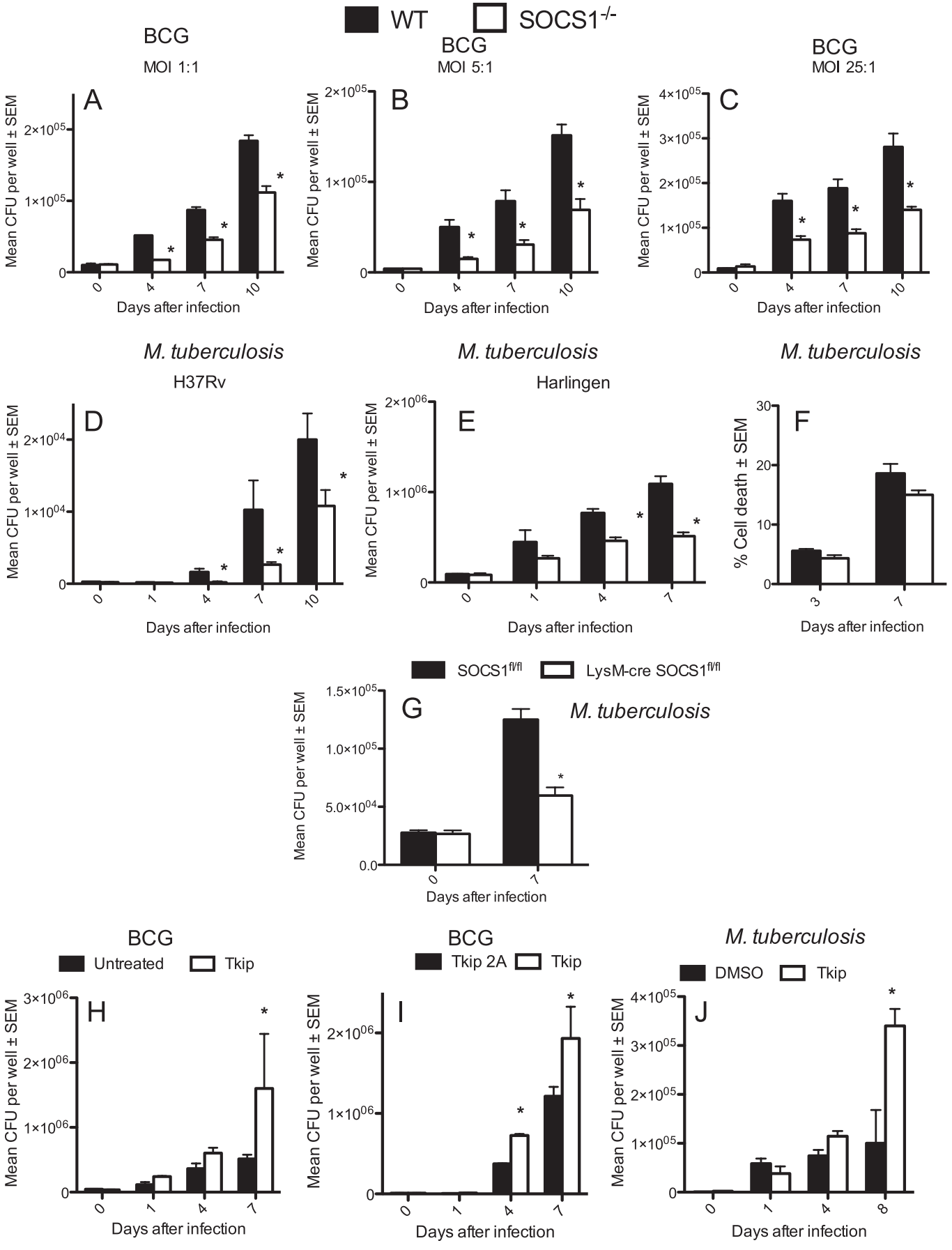
WT
SOCS1-/-
BCG
MOI 1:1
A
Mean CFU per well ± SEM
Days after infection
BCG
MOI 5:1
B
BCG
MOI 25:1
C
M. tuberculosis
H37Rv
D
M. tuberculosis
Harlingen
E
M. tuberculosis
F
% Cell death ± SEM
SOCS1fl/fl
LysM-cre SOCS1fl/fl
G
M. tuberculosis
BCG
Untreated
Tkip
H
BCG
Tkip 2A
Tkip
I
M. tuberculosis
DMSO
Tkip
J

tin (1:500 dilution; Sigma). Membranes were then washed and incubated with horseradish peroxidase (HRP)-conjugated polyclonal goat anti-rabbit immunoglobulin (1:2000 dilution; DAKO, Glostrup, Denmark) and developed using ECL-Plus (Amersham Biosciences) and photographed using a Fuji intelligent dark box II digital camera.

Microarray Analysis—The RNA was labeled using QuickAmp labeling kit (Agilent Technologies, Santa Clara, CA) according to the manufacturer's instructions. The Cy3-labeled cRNA was hybridized to Whole Mouse Genome Microarrays (Agilent), and the Agilent "Feature Extraction" software was used to extract data. The analysis included four arrays on a chip per sample. The data array consisted of infected or uninfected WT and *SOCS1*$^{-/-}$ BMM. The data were normalized in GeneSpring GX by setting threshold raw signal to 1 for the median of control samples. Base line was set to the median of all the samples. Of 41,252 probes, 37,469 probes passed filtered on expression 20–100th percentile in the raw data, of which 30,127 were flagged by software as present or marginally present in at least one condition. The microarray data were deposited in the GEO data base, accession number GSE23508.

Enzyme-linked Immunosorbent Spot Assay—For the IFN-γ ELISPOT assay, 10^5 BMDC were infected with BCG and plated in triplicates in 96-well nitrocellulose-bottomed plates previously coated with 5 μg/ml anti-mouse IFN-γ mAb AN18 (MabTech AB, Sweden). Plates were incubated for 20 h at 37 °C. Biotinylated detector antibody (R4-6A2, MabTech) was added for 2 h and incubated at room temperature. Afterward, plates were washed and incubated for 1 h in the dark with 100 μl of avidin-peroxidase complexes (ABC-elite kit, Vector Laboratories, Burlingame, CA). The spots were developed by adding 20 mg of 3-amino-9-ethylcarbozole (Sigma) dissolved in 2.5 ml of dimethylformamide in 47.5 ml of acetate buffer containing 0.015% H_2O_2.

Intracellular Cytokine Staining—Lungs were perfused with PBS through the heart before removal from mice. Following digestion with collagenase D and DNase I, erythrocytes were lysed, and single-cell suspensions were prepared by filtering lung tissue through 40-μm nylon cell strainers. Single spleen cell suspensions were obtained, and red blood cells were lysed. 10^6 cells were stimulated with 20 μg/ml PPD (Statens Serum Institute, Copenhagen, Denmark) overnight, followed by a 6-h incubation with brefeldin A (5 μg/ml). To determine the percentages of IFN-γ-secreting T-cells, we first stained with anti-mouse CD4 eFluor®450 (eBioscience, San Diego, CA) and CD3ϵ PerCP (BD Pharmingen, San Diego, CA) and then permeabilized the cells using leukocytic permeabilization reagent IntraPrep™ (Beckman Coulter) and stained them with anti-IFN-γ APC (eBioscience). Data were acquired in a CyAn™ ADP flow cytometer (Beckman Coulter) and analyzed using FlowJo software (Tree Star Inc., Ashland, OR).

RESULTS

Expression of SOCS1 mRNA in BCG-infected Macrophages Requires Phagocytosis and the Presence of Innate TLR, NOD2, and IFN-α/β Receptors—In a first set of experiments, regulation of *SOCS1* gene expression in macrophages infected with mycobacteria was studied. *SOCS1* mRNA accumulation increased in BMM infected with BCG (Fig. 1*A*). In order to determine whether phagocytosis was required for SOCS1 expression, macrophages were treated with cytochalasin D, an inhibitor of actin polymerization. Cytochalasin D-treated BMM showed lower *SOCS1* mRNA levels than untreated controls (Fig. 1*A*). As a control, similar levels of *SOCS1* mRNA after incubation with a TLR agonist binding to cell surface receptors were measured in cells treated or not with cytochalasin D (supplemental Fig. S1*A*).

We then asked whether MyD88- and IRF3-mediated intracellular signaling pathways are involved in the augmented *SOCS1* mRNA levels after infection with BCG. Similar *SOCS1* mRNA levels were found in BCG-infected *IRF3*$^{-/-}$ and wild type (WT) BMM, whereas infected *MyD88*$^{-/-}$ BMM displayed significantly lower *SOCS1* mRNA levels than controls (Fig. 1*B*). Because TLR2 and -4 have been shown to recognize mycobacterial components and mediate MyD88-dependent macrophage responses to infection (40–42), the role of these TLR in SOCS1 regulation during mycobacterial infection was studied. *SOCS1* mRNA levels were diminished in *TLR2*$^{-/-}$ BMM, albeit to a lower degree than in *MyD88*$^{-/-}$ BMM (Fig. 1*C*). In line with this, stimulation of BMM with the TLR2 agonist Pam3 was sufficient to induce *SOCS1* mRNA (Fig. 1*D*). In contrast, TLR4 seemed to play a minor role if any in regulation of *SOCS1* mRNA levels in BCG-infected macrophages (Fig. 1*C*).

The NOD2 pathway is also involved in mycobacterial recognition (43). Diminished levels of *SOCS1* mRNA were observed in *NOD2*$^{-/-}$ BCG-infected BMM, compared with WT controls (Fig. 1*E*).

Both TLR and NOD pathways will trigger activation of NF-κB. Co-incubation of BCG-infected BMM with BAY 11-7082, a pharmacological inhibitor of IκB-α phosphorylation, reduced the relative levels of *SOCS1* mRNA (Fig. 1*F*). As expected, the NF-κB-dependent *MCP-1* but not *IFN-α* mRNA levels were reduced in BAY 11-7082-treated BCG-infected BMM (supplemental Fig. S1*B*) (data not shown). IFN-α/β are also involved in *SOCS1* mRNA expression during infection because *IFN-α/βR*$^{-/-}$ BMM showed lower levels of SOCS1 compared with WT controls (Fig. 1*G*).

Induction of *SOCS1* mRNA after infection with BCG and *M. tuberculosis* was then compared. Murine BMM and human

FIGURE 2. **SOCS1 hinders growth control of BCG and *M. tuberculosis* by macrophages.** *RAG1*$^{-/-}$/*SOCS1*$^{+/+}$ and *RAG1*$^{-/-}$/*SOCS1*$^{-/-}$ BMM, (indicated hereafter as WT and *SOCS1*$^{-/-}$) were infected with different MOI of BCG (*A–C*) or *M. tuberculosis* H37Rv (*D*) or Harlingen (*E*) at an MOI of 5:1, washed after 2 h, and lysed with PBS-Triton buffer at the indicated time points after infection. The cfu were determined in triplicate cell cultures. At least two independent experiments for each panel were performed. The content of lactate dehydrogenase in supernatants from *M. tuberculosis* Harlingen-infected *SOCS1*$^{-/-}$ and WT BMM at an MOI of 5:1 was measured as assessment of cell damage. The mean percentage lysis ± S.E. (*error bars*) in triplicate cultures with respect to cells incubated with 1% Triton X-100 is depicted (*F*). *LysM-cre SOCS1*$^{fl/fl}$ and *SOCS1*$^{fl/fl}$ BMM were infected with *M. tuberculosis* in triplicate cell cultures at an MOI of 1:1. The cfu in lysates were determined. At least two independent experiments for each panel were performed (*G*). BMM were treated with 30 μM lipophilic JAK2 tyrosine kinase inhibitor peptide (Tkip) (*H–J*) or with a Tkip2A (*I*), an alanine substitution-containing mutant form of Tkip that does not show any biological activity. Peptides were added 30 min before infection with BCG (*H* and *I*) or *M. tuberculosis* H37Rv (*J*) and replenished after cells were extensively washed, 2 h after bacterial co-incubation. Control infected cells were incubated with DMSO (*H* and *J*). The mean cfu ± S.E. were determined in triplicate cell cultures from at least two independent experiments. *, differences with control BMM are significant ($p < 0.05$, Student's *t* test).

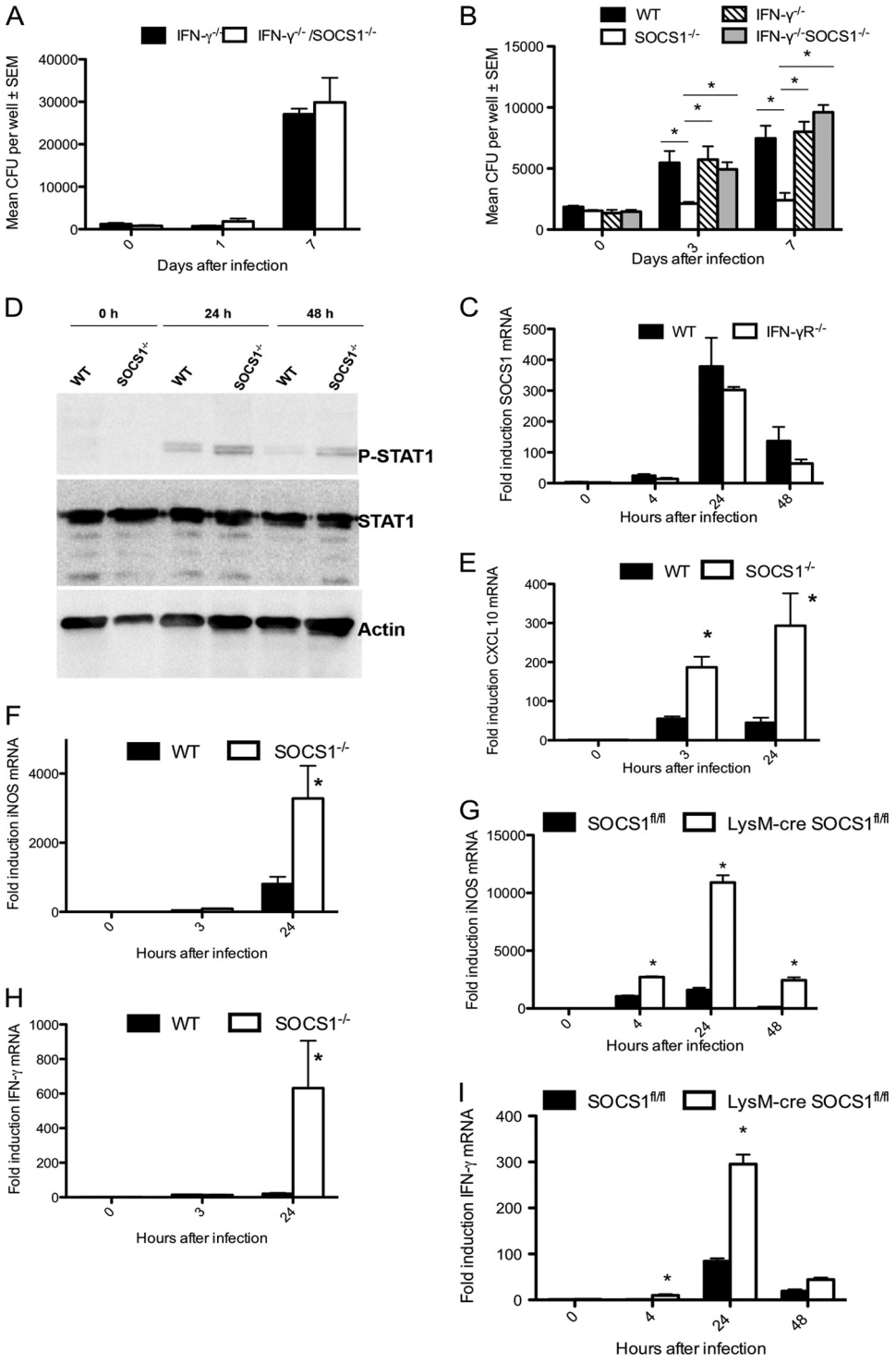

FIGURE 3. **SOCS1 hinders clearance of *M. tuberculosis* by macrophages in an IFN-γ-mediated manner.** *IFN-*$\gamma^{-/-}$ and *IFN-*$\gamma^{-/-}$*/SOCS1*$^{-/-}$ BMM were infected with BCG at MOI 1:1 (*A*). WT, *SOCS1*$^{-/-}$, *IFN-*$\gamma^{-/-}$ and *IFN-*$\gamma^{-/-}$*/SOCS1*$^{-/-}$ BMM were infected with *M. tuberculosis* H37Rv at an MOI of 1:1 (*B*). The cfu were determined in lysates from triplicate cultures (*A* and *B*). The mean cfu/well ± S.E. (*error bars*) from one of two independent experiments is depicted. Total RNA was isolated from *IFN-*$\gamma R^{-/-}$ and WT BMM at different time points after infection with *M. tuberculosis* H37Rv at an MOI of 5:1 (*C*). The accumulation of SOCS1 and *Hprt* mRNA was measured by real-time PCR. Protein extracts from WT and *SOCS1*$^{-/-}$ BMM were prepared at the indicated time points after infection with *M. tuberculosis* and separated by SDS-PAGE, and phosphorylated STAT1, total STAT1, and actin were detected by Western blot (*D*). Total RNA was extracted from *SOCS1*$^{-/-}$ and WT (*E*, *F*, and *H*) or *LysM-cre SOCS1*$^{fl/fl}$ and *SOCS1*$^{fl/fl}$ (*G* and *I*) BMM at the indicated time points after infection with *M. tuberculosis* H37Rv. The relative concentrations of CXCL10 (*E*), iNOS (*F* and *G*), IFN-γ (*H* and *I*), and *Hprt* mRNA were determined by real-time PCR. The mean -fold induction of these transcripts ± S.E. is depicted. *, differences with control BMM are significant ($p < 0.05$ Student's *t* test).

monocyte-derived macrophages expressed higher titers of *SOCS1* mRNA after infection with *M. tuberculosis* than BCG (Fig. 1, *H* and *I*).

SOCS1 Hampers Efficient Growth Control of Intracellular BCG and M. tuberculosis by Macrophages—Next, we investigated whether SOCS1 plays a role in intracellular growth con-

trol of BCG. *SOCS1*$^{-/-}$ and WT BMM were infected with BCG. *SOCS1*$^{-/-}$ BMM infected at different MOI showed reduced bacterial load (Fig. 2, *A*–*C*) compared with WT controls. Accordingly, *SOCS1*$^{-/-}$ BMM showed lower levels of *M. tuberculosis* H37Rv or Harlingen than WT cells (Fig. 2, *D* and *E*). Similar levels of *SOCS1*$^{-/-}$ and WT BMM death were recorded during *M. tuberculosis* infection as measured by release of lactate dehydrogenase into the medium (Fig. 2*F*).

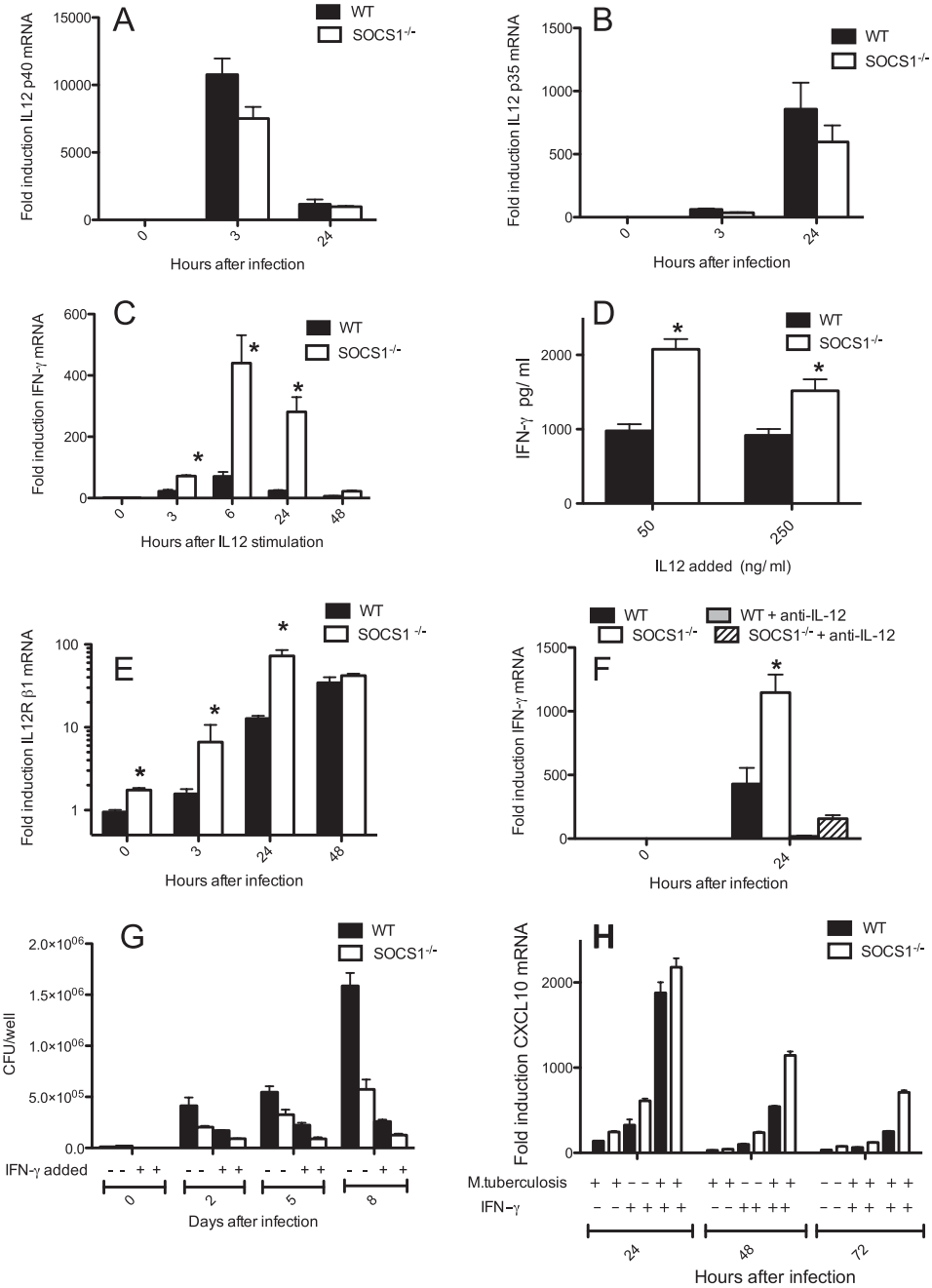

The *SOCS1* gene was deleted in macrophages and neutrophils by crossing $SOCS1^{fl/fl}$ mice with *LysM-cre* $SOCS1^{fl/fl}$ mice. Infected *LysM-cre* $SOCS1^{fl/fl}$ BMM also showed reduced *M. tuberculosis* levels compared with $SOCS1^{fl/fl}$ controls (Fig. 2*G*). *SOCS1* mRNA levels in *LysM-cre* $SOCS1^{fl/fl}$ were 40–300-fold lower than the controls. The remnant expression is probably due to non-macrophage cells in the BMM cultures or to incomplete deletion of SOCS1 in *LysM-cre* $SOCS1^{fl/fl}$ BMM (supplemental Fig. S2*A*). Altogether, we confirm that SOCS1-silenced BMM show decreased *M. tuberculosis* levels.

In agreement, increased bacterial growth was observed upon incubation of BCG or *M. tuberculosis*-infected BMM with Tkip, a 12-mer peptide that, similar to SOCS1, binds and inhibits autophosphorylation of the JAK2 kinase and phosphorylation of the intracellular IFN-γ receptor (44) (Fig. 2, *H*–J). BMM treated with a Tkip-related peptide (alanine substituted by phenylalanine at positions 8 and 11, abrogating thereby binding to JAK2 (45)) showed lower bacterial levels than those treated with the native peptide (Fig. 2*I*). As shown previously (44), incubation of BMM with Tkip during stimulation with recombinant IFN-γ diminished pSTAT1 levels (data not shown).

SOCS1 Inhibits IFN-γ Secretion and Thereby Precludes Efficient Clearance of BCG and M. tuberculosis in Macrophages—BCG-infected $SOCS1^{-/-}$ BMM (supplemental Fig. S2, *B–D*) and BMDC (supplemental Fig. S2, *E–G*) showed increased levels of *IFN-β* (supplemental Fig. S2, *B* and *E*), *IFN-α* (supplemental Fig. S2, *C* and *F*) and *IFN-γ* (supplemental Fig. S2, *D* and *G*) mRNA as compared with WT BMM. Also, the frequency of IFN-γ-secreting BCG-infected $SOCS1^{-/-}$ BMDC was higher than WT controls (supplemental Fig. S2*H*).

Because IFN-γ controls macrophage activation and mycobacterial growth, we studied whether the improved mycobacterial growth control in $SOCS1^{-/-}$ BMM is IFN-γ-dependent. For this purpose, titers of *M. tuberculosis* and BCG in $IFN\text{-}\gamma^{-/-}/SOCS1^{-/-}$ and $IFN\text{-}\gamma^{-/-}$ BMM were compared. $IFN\text{-}\gamma^{-/-}/SOCS1^{-/-}$ and $IFN\text{-}\gamma^{-/-}$ BMM showed similar BCG loads (Fig. 3*A* and supplemental Fig. S2*I*). Moreover, similar bacterial levels were measured in WT, $IFN\text{-}\gamma^{-/-}$, and $IFN\text{-}\gamma^{-/-}/SOCS1^{-/-}$ *M. tuberculosis*-infected BMM, whereas the bacterial load in $SOCS1^{-/-}$ BMM was lower compared with all other groups (Fig. 3*B*). Altogether, these results indicate that SOCS1 inhibits secretion of IFN-γ that otherwise would mediate a more effective clearance of mycobacteria in macrophages.

Whether infection-stimulated SOCS1 expression is IFN-γ-dependent was next investigated. We found that IFN-γ was not required for SOCS1 expression because similar levels of *SOCS1* mRNA were detected in BCG- or *M. tuberculosis*-infected WT and $IFN\text{-}\gamma R^{-/-}$-deficient BMM (Fig. 3*C* and supplemental Fig. S2*J*).

Infection of BMM with *M. tuberculosis* led to STAT1 activation as measured by phosphorylation of the transcription factor. Higher levels of pSTAT1 were observed in $SOCS1^{-/-}$ compared with WT BMM when measured 24 and 48 h after infection (Fig. 3*D*). In agreement with higher levels of STAT1 activation, the titer of the STAT1-regulated *CXCL10* and *iNOS* transcripts were increased in *M. tuberculosis*-infected $SOCS1^{-/-}$ as compared with respective controls (Fig. 3, *E* and *F*). Moreover and similar to observations in BCG-infected BMM, the level of *IFN-γ* mRNA was augmented in *M. tuberculosis*-infected $SOCS1^{-/-}$ BMM (Fig. 3*H*). Both *iNOS* and *IFN-γ* mRNA levels were higher in *LysM-cre* $SOCS1^{fl/fl}$ BMM compared with controls (Fig. 3, *G* and *I*), confirming that SOCS1 expression in macrophages hampers IFN-γ expression.

Because IL-12 is known to be a main stimulus for IFN-γ secretion, we next investigated whether an *M. tuberculosis*-induced SOCS1-diminished expression of IL-12 could account for the increased IFN-γ secretion in $SOCS1^{-/-}$ BMM. However, similar mRNA levels of *IL-12 p35* and *IL-12 p40*, constituents of biologically active IL-12 dimers, were found in *M. tuberculosis*-infected $SOCS1^{-/-}$ and WT BMM (Fig. 4, *A* and *B*), suggesting that the response to but not the secretion of IL-12 could account for the increased IFN-γ release in $SOCS1^{-/-}$ BMM. In order to test this hypothesis, the concentration of *IFN-γ* mRNA and protein was measured in WT and $SOCS1^{-/-}$ BMM stimulated with recombinant IL-12. $SOCS1^{-/-}$ BMM stimulated with IL-12 contained enhanced *IFN-γ* mRNA and protein levels compared with WT controls (Fig. 4, *C* and *D*).

The increased response to IL-12 of $SOCS1^{-/-}$ BMM was associated with higher levels of the *IL-12Rβ1* (IL-12 receptor β1) but not *IL-12Rβ2* mRNA in both *M. tuberculosis*-infected and uninfected $SOCS1^{-/-}$ compared with WT BMM (Fig. 4*E*) (data not shown).

The effect of IL-12 neutralization in IFN-γ expression by *M. tuberculosis*-infected $SOCS1^{-/-}$ BMM was then studied. The addition of anti-IL-12 antibodies reduced *IFN-γ* mRNA levels in *M. tuberculosis*-infected $SOCS1^{-/-}$ and WT BMM (Fig. 4*F*), indicating that IL-12 is required for the enhanced IFN-γ secretion by the infected $SOCS1^{-/-}$ BMM.

FIGURE 4. **SOCS1 inhibits response to but not the secretion of IL-12, does not hamper responses to IFN-γ, and regulates the global transcriptional responses to infection of macrophages with *M. tuberculosis*.** Total RNA was extracted from $SOCS1^{-/-}$ and WT BMM at the indicated time points after infection with *M. tuberculosis* H37Rv (*A*, *B*, *E*, and *F*) or after stimulation with 20 ng/ml recombinant IL-12 p70 (*C*). The accumulation of IL-12 p40 (*A*), IL-12 p35 (*B*), IFN-γ (*C* and *F*), IL-12Rβ1 (*E*), and *Hprt* mRNA was measured by real time PCR. The mean -fold accumulation of the transcripts of triplicate cultures per time point in relation to *Hprt* ± S.E. (*error bars*) is depicted. The level of IFN-γ in the supernatant of triplicate cultures of IL-12-stimulated $SOCS1^{-/-}$ or WT BMM was measured by ELISA (*D*). *, differences with control BMM are significant ($p < 0.05$, Student's *t* test). The levels of IFN-γ mRNA in $SOCS1^{-/-}$ and WT BMM incubated or not with 10 μg/ml anti-p40/p70 IL-12-neutralizing antibodies (BD Biosciences) 1 h before infection with *M. tuberculosis* (*F*) were determined as described above. Twenty-four h after infection with *M. tuberculosis*, $SOCS1^{-/-}$ or WT BMM were co-incubated with 100 units of recombinant IFN-γ or left untreated. The number of cfu ± S.E. in lysates from triplicate cultures at each time point after infection is depicted (*G*). $SOCS1^{-/-}$ and WT BMM were treated with IFN-γ 24 h after infection with *M. tuberculosis*. Infected and mock controls were harvested at the indicated time points after infection. The accumulation of *CXCL10* (*G*) and *Hprt* mRNA was measured by real-time PCR. The mean -fold accumulation of *CXCL10* mRNA of triplicate cultures per time point in relation to *Hprt* ± S.E. is depicted (*H*). Differences between IFN-γ-treated and untreated cells are significant ($p < 0.05$, Student's *t* test). To obtain the microarray data, RNA was isolated from *M. tuberculosis*-infected or uninfected, WT or $SOCS1^{-/-}$ BMM cultures, with four independent samples in each group. The Venn diagram illustrates the number of genes altered by pathogen exposure (independently of the genotype) or differentially expressed by $SOCS1^{-/-}$ and WT BMM (independently of infection) (*I*). The statistical significance of differentially expressed probes was identified by two-way analysis of variance ($p < 0.05$), including the Benjamini and Hochberg false discovery rate correction (5%).

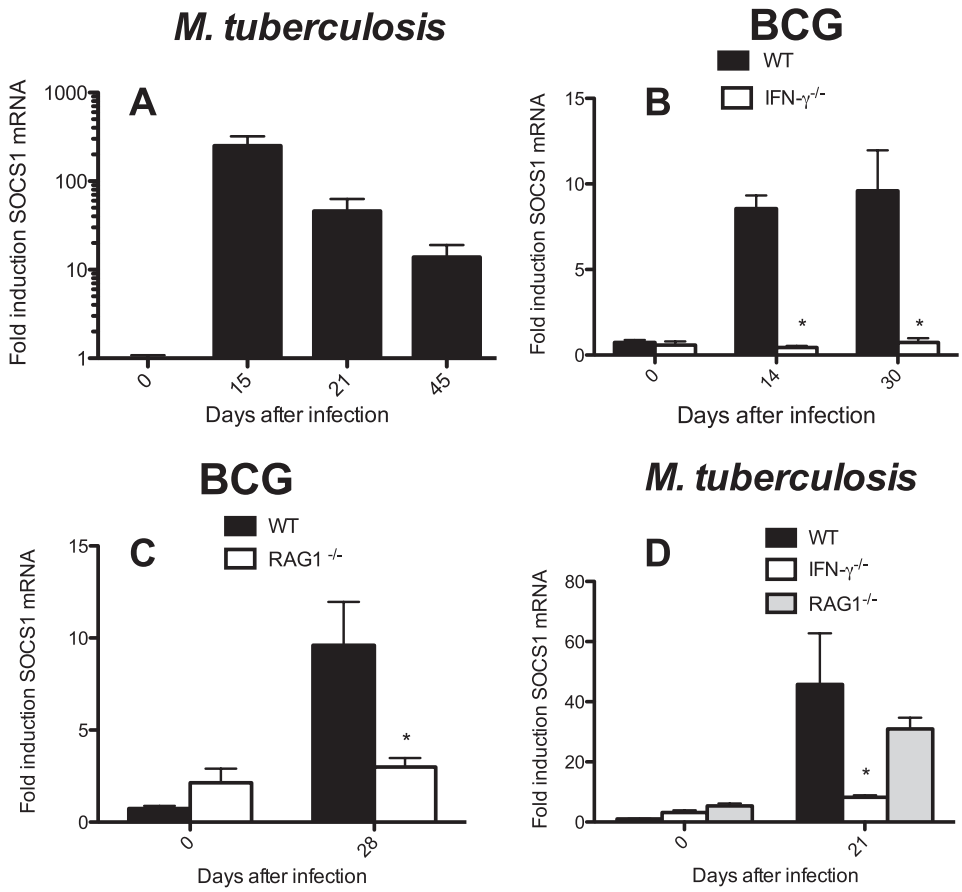

FIGURE 5. **IFN-γ-dependent control of *SOCS1* mRNA levels in lungs from mice infected with *M. tuberculosis* or BCG.** Total RNA was extracted from lungs of individual WT (*A–D*), *IFN-γ*$^{-/-}$ (*B* and *D*), *RAG1*$^{-/-}$ (*C* and *D*) mice after infection intravenously with 10^6 BCG (*B* and *C*) or via the aerosol route with 250 *M. tuberculosis* Harlingen strain (*D*). The mean -fold accumulation of SOCS1 transcripts ± S.E. (*error bars*) in lungs from infected mice ($n \geq 5$ mice/infected group) is depicted. *, differences with WT-infected mice in *B–D* are significant ($p < 0.05$, Student's *t* test).

We then studied if the increased responses to IL-12 of *SOCS1*$^{-/-}$ BMM are due to uncontrolled IL-12 signaling and/or to increased IL-12R expression. We found that *IL-12Rβ1* mRNA accumulation in *M. tuberculosis*-infected *IFN-γ*$^{-/-}$ and *IFN-γ*$^{-/-}$/*SOCS1*$^{-/-}$ BMM was similar (supplemental Fig. S3*A*). This result suggests that hyperresponses to IL-12 during infection of *SOCS1*$^{-/-}$ BMM are primarily due to an intrinsically increased IL-12 signaling because *IL-12Rβ1* expression is IFN-γ-dependent.

Whether SOCS1 further impedes the responses of *M. tuberculosis*-infected BMM to IFN-γ was then studied. Incubation of either *SOCS1*$^{-/-}$ or WT BMM with IFN-γ 24 h after infection with *M. tuberculosis* resulted in diminished bacterial load as compared with respective IFN-γ-untreated infected controls (Fig. 4*G*). Endorsing the previous result, *CXCL10* or *iNOS* mRNA levels were increased in IFN-γ-treated, infected WT or *SOCS1*$^{-/-}$ BMM cells as compared with uninfected controls or with infected cells in the absence of IFN-γ stimulation. Uninfected *SOCS1*$^{-/-}$ BMM showed higher levels of *CXCL10* mRNA after stimulation with IFN-γ as compared with WT controls (Fig. 5*H*) (data not shown). NO is generated by iNOS, which requires both NF-κB and STAT1 for its activation, explaining thereby the lack of *iNOS* mRNA expression in uninfected, IFN-γ-treated WT or *SOCS1*$^{-/-}$ BMM (supplemental Fig. S3*C*). Of importance, levels of *CXCL10* and *iNOS* mRNA were higher in *SOCS1*$^{-/-}$ BMM stimulated or not with IFN-γ 3 or 24 h after infection with *M. tuberculosis*, as compared with the respective WT control (Fig. 4*H* and supplemental Fig. S3, *B* and *C*).

SOCS1 Regulates the Macrophage Global Transcriptional Responses to Infection with M. tuberculosis—To investigate how SOCS1 shapes the macrophage response to *M. tuberculosis* at the transcriptome level, a genome-wide expression analysis was performed. For this purpose, total RNA was isolated from *M. tuberculosis*-infected or uninfected *SOCS1*$^{-/-}$ and WT BMM, and cRNA was transcribed, labeled, and hybridized to genome-wide high density microarrays. The expression levels of 1430 genes, or 6.1% of the mouse genome, differed in the infected compared with uninfected BMM, independent of their genotype. From these genes, 1365 tally within the 1904 genes differentially regulated in *SOCS1*$^{-/-}$ compared with WT BMM (independent of their infection status) (Fig. 4*I*). The majority, 987 genes, showed diminished levels of expression in *SOCS1*$^{-/-}$-infected compared with WT-infected BMM, whereas 371 were increased in *SOCS1*$^{-/-}$-infected BMM. Moreover, titers of 1804 genes diverged in *SOCS1*$^{-/-}$ compared with WT-infected BMM. 1306 genes from this subgroup were regulated by *M. tuberculosis* infection and the genotype.

Differences in levels of 40 IFN-regulated transcripts were found in *SOCS1*$^{-/-}$- compared with WT-infected BMM (Table

TABLE 1

IFN-regulated genes in *M. tuberculosis*-infected SOCS1$^{-/-}$ and WT BMM

Shown are genes significantly increased or decreased due to the genotype and the infection (two-way analysis of variance, $p < 0.05$) and further selected for a -fold difference between *M. tuberculosis*-infected SOCS1$^{-/-}$ and WT BMM of ≥2. The selection was made with regard to the GO annotation and their known function. The ratios of housekeeping gene-normalized mean levels of transcripts selected, in SOCS1$^{-/-}$ and WT-uninfected BMM, and of infected and uninfected WT BMM are also shown.

Gene symbols and functions	Description	SOCS1 KO-infected/ WT-infected	SOCS1 KO-uninfected/ WT-uninfected	WT-infected/ WT-uninfected
Effector mechanisms and unknown functions				
Iigp2	Interferon-inducible GTPase 2	2.08	1.00	1.90
Ifih1	Interferon induced with helicase C domain 1	2.20	1.00	2.90
Ifi202b	Interferon-activated gene 202B	2.28	1.21	13.30
Gvin1	GTPase, very large interferon-inducible 1	2.38	1.04	1.82
Ifi47	Interferon γ-inducible protein 47	2.65	1.04	3.10
Ifi203	Interferon-activated gene 203	2.84	1.21	1.30
Ifi205	Interferon-activated gene 205	2.93	0.96	41.86
Ifit1	Interferon-induced protein with tetratricopeptide repeats 1	4.59	1.03	7.19
Ifit2	Interferon-induced protein with tetratricopeptide repeats 2	3.20	0.83	3.68
Ifit3	Interferon-induced protein with tetratricopeptide repeats 3	3.30	0.95	3.17
Iigp1	Interferon-inducible GTPase 1	4.85	1.13	3.89
Ifi44	Interferon-induced protein 44	5.01	1.02	6.70
Eg240921	Interferon-inducible protein p204	5.70	1.11	5.90
Mpa2l	Macrophage activation 2-like	2.03	1.08	23.18
Noxa1	NADPH oxidase activator 1	2.02	1.50	3.02
Defb11	Defensin β 11	2.26	1.04	0.49
Stat1	Signal transducer and activator of transcription 1	2.25	1.00	3.38
Irg1	Immunoresponsive gene 1	3.31	1.10	178.28
Antigen presentation				
Cd1d1	CD1d1 antigen	2.30	1.01	3.13
Cd1d2	CD1d2 antigen	3.61	1.42	3.09
H2-T24	Histocompatibility 2, T region locus 24	2.29	0.92	6.08
Cd86	CD86 antigen	2.29	1.04	1.56
Ciita	Class II transactivator	0.43	1.07	0.27
Cytokine and chemokines, receptors, SOCS				
Socs1	Suppressor of cytokine signaling 1			73.04
Socs3	Suppressor of cytokine signaling 3	2.07	1.05	131.15
Cish	Cytokine-inducible Src homology 2-containing protein	2.45	0.89	51.10
Ifng	Interferon γ	5.95	1.23	10.66
Il12rb1	Interleukin 12 receptor, β 1	3.19	1.36	14.00
Il1b	Interleukin 1 β (Il1b), mRNA	4.08	1.00	97.05
Cxcr3	Chemokine (CXC motif) receptor 3	0.36	1.02	0.46
Cxcl9	Chemokine (CXC motif) ligand 9	4.81	0.86	9.93
Cxcl10	Chemokine (CXC motif) ligand 10	4.32	1.08	16.58
Type I IFN-stimulated genes				
Isg15	ISG15 ubiquitin-like modifier	3.54	1.03	15.11
Ifnb1	Interferon β 1, fibroblast	5.33	1.18	25.49
Oas1g	2′-5′ oligoadenylate synthetase 1	2.27	0.93	23.25
Oasl2	2′-5′ oligoadenylate synthetase-like 2	2.45	0.95	2.90
Oas2	2′-5′ oligoadenylate synthetase 2	3.00	1.06	1.44
Gbp5	Guanylate nucleotide binding protein 5	2.48	0.92	8.20
Mx1	Myxovirus (influenza virus) resistance 1	3.39	1.06	4.60
Mx2	Myxovirus (influenza virus) resistance 2	3.40	1.04	4.86
Ddx58	DEAD (Asp-Glu-Ala-Asp) box polypeptide 58 (Ddx58)	2.27	1.03	2.92

1). Thirty-eight of these transcripts, involved in antigen presentation, chemotaxis, and effector mechanisms, were increased in the *SOCS1*$^{-/-}$-infected BMM, whereas only two were found to be reduced (Table 1). IFN-γ- and IFN-β-regulated as well as IFN-α/β-regulated transcripts were increased in *M. tuberculosis*-infected *SOCS1*$^{-/-}$ BMM (Table 1). The differences recorded are a consequence of *M. tuberculosis* infection because levels of these transcripts in WT and *SOCS1*$^{-/-}$ BMM before infection were similar. Moreover, *M. tuberculosis* induced expression of the selected IFN-regulated genes because 34 of these transcripts were increased in infected compared with uninfected WT BMM, whereas none decreased after infection (Table 1).

Higher Levels of SOCS1 mRNA after Infection in Vivo with M. tuberculosis—Levels of *SOCS1* mRNA in lung cells from WT mice infected with *M. tuberculosis* or BCG were augmented as compared with uninfected controls (Fig. 5*A*) (data not shown).

SOCS1 mRNA levels were, on the contrary, not increased in lungs from BCG-infected *RAG1*$^{-/-}$ or *IFN-γ*$^{-/-}$ mice (Fig. 5, *B* and *C*). This suggests that IFN-γ secretion and adaptive immune cells are required for the elevated *SOCS1* mRNA levels registered after BCG infection in WT mice. *SOCS1* transcript titers in lungs from *M. tuberculosis*-infected *IFN-γ*$^{-/-}$ and *IFN-γR*$^{-/-}$ but not *RAG-1*$^{-/-}$ mice were lower than in WT-infected controls (Fig. 5*D*). On the other hand, *SOCS1* mRNA was increased in *RAG1*$^{-/-}$ and *IFN-γ*$^{-/-}$ mice compared with uninfected controls (supplemental Fig. S4, *D* and *E*).

SOCS1 Expression in Macrophages Hampers M. tuberculosis Control Early after Infection—Whether SOCS1 could affect the outcome of mycobacterial infection *in vivo* was next explored.

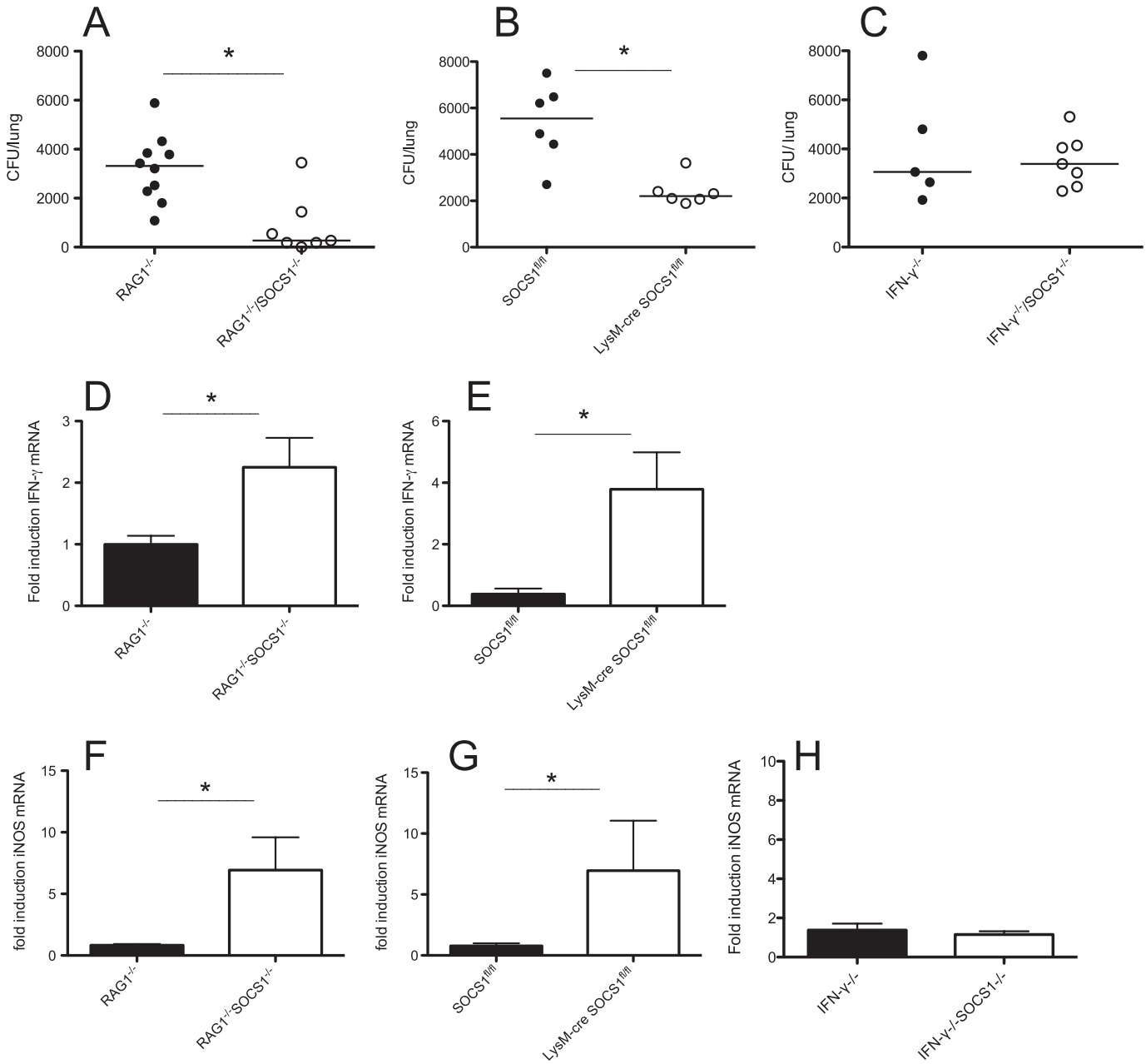

FIGURE 6. **Reduced bacterial load and increased IFN-γ and iNOS mRNA in *M. tuberculosis*-infected SOCS1-deficient mice.** *RAG1*$^{-/-}$ *SOCS1*$^{-/-}$, *RAG1*$^{-/-}$ (*A*, *D*, and *F*), *LysM-cre SOCS1*$^{fl/fl}$, *SOCS1*$^{fl/fl}$ (*B*, *E*, and *G*), *IFN-γ*$^{-/-}$/*SOCS1*$^{-/-}$, and *IFN-γ*$^{-/-}$ (*C* and *H*) mice were infected with *M. tuberculosis* H37Rv via the aerosol route. Animals were sacrificed 1 week after infection, and cfu per lung and spleen were assessed. The cfu/lung of individual mice and the median/group at the indicated time points after infection are depicted (*A–C*). *, differences in cfu are significant ($p < 0.05$, Mann-Whitney *U* test). Total RNA was extracted from lungs, and the mean -fold accumulation of *IFN-γ* (*D* and *E*) and *iNOS* (*F–H*) transcripts ± S.E. (*error bars*) in lungs from infected mice ($n \geq 5$/group) was calculated. *, differences with controls are significant ($p < 0.05$, Student's *t* test).

We found lower bacterial levels in lungs of both *LysM-cre SOCS1*$^{fl/fl}$ and *RAG1*$^{-/-}$/*SOCS1*$^{-/-}$ mice 7 days after aerosol infection with 250 *M. tuberculosis* bacteria in comparison with respective controls (Fig. 6, *A* and *B*). On the contrary, similar bacterial titers were measured in lungs from *IFN-γ*$^{-/-}$/*SOCS1*$^{-/-}$ and *IFN-γ*$^{-/-}$ mice (Fig. 6*C*). Dissemination of bacteria to the spleen remained undetectable at this time point.

In agreement with *in vitro* data, lungs from *RAG1*$^{-/-}$/*SOCS1*$^{-/-}$- and *LysM-cre SOCS1*$^{fl/fl}$-infected mice showed higher accumulation of both *IFN-γ* and *iNOS* transcripts compared with controls (Fig. 6, *D–G*). In contrast there was no enhanced accumulation of *iNOS* transcripts in *IFN-γ*$^{-/-}$/*SOCS1*$^{-/-}$- and *IFN-γ*$^{-/-}$-infected mice compared with uninfected controls (Fig. 6*H*).

Increased Severity of Pulmonary Inflammation in SOCS1$^{-/-}$ *Mice*—On the other hand, lungs and spleens from *LysM-cre SOCS1*$^{fl/fl}$ and *RAG1*$^{-/-}$/*SOCS1*$^{-/-}$ mice showed no reduction of the bacterial numbers at later time points after infection (Fig. 7, *A* and *H*). Increased levels of *IFN-γ* and *iNOS* mRNA were measured in lungs from *RAG1*$^{-/-}$ and *RAG1*$^{-/-}$/*SOCS1*$^{-/-}$ at 3 weeks after infection as compared with uninfected controls. However, titers of *IFN-γ* and *iNOS* mRNA in lungs from

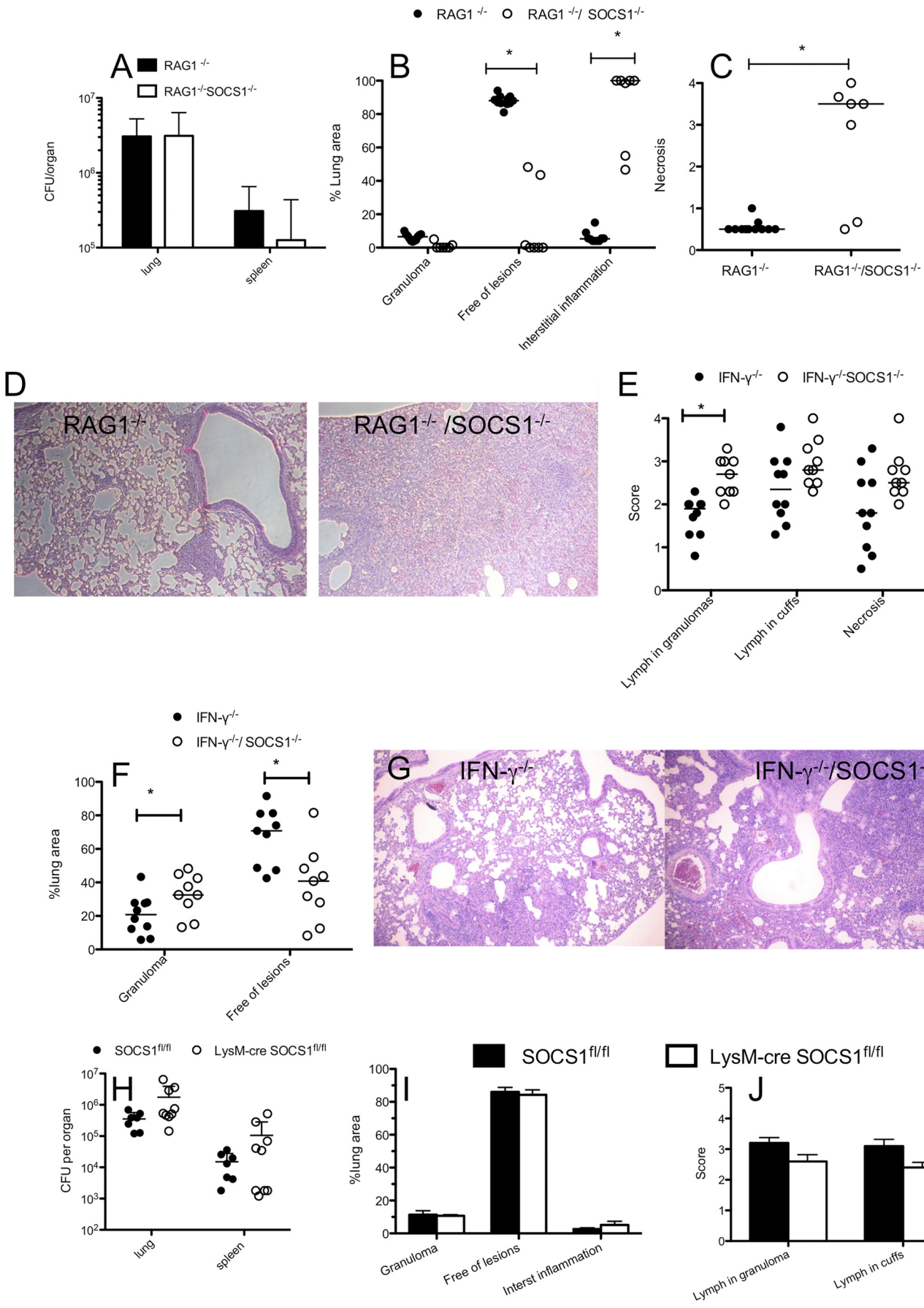
A
RAG1 -/-
RAG1-/-SOCS1-/-
CFU/organ
lung
spleen
B
RAG1 -/-
RAG1 -/-/ SOCS1-/-
% Lung area
Granuloma
Free of lesions
Interstitial inflammation
C
Necrosis
RAG1-/-
RAG1-/-/SOCS1-/-
D
RAG1-/-
RAG1-/- /SOCS1-/-
E
IFN-γ-/-
IFN-γ-/-SOCS1-/-
Score
Lymph in granulomas
Lymph in cuffs
Necrosis
F
IFN-γ-/-
IFN-γ-/-/ SOCS1-/-
%lung area
Granuloma
Free of lesions
G
IFN-γ-/-
IFN-γ-/-/SOCS1-/-
H
SOCS1fl/fl
LysM-cre SOCS1fl/fl
CFU per organ
lung
spleen
I
SOCS1fl/fl
LysM-cre SOCS1fl/fl
%lung area
Granuloma
Free of lesions
Interst inflammation
J
Score
Lymph in granuloma
Lymph in cuffs

RAG1$^{-/-}$/*SOCS1*$^{-/-}$ and *RAG1*$^{-/-}$ mice were similar (supplemental Fig. S4, *A* and *B*). We then asked whether SOCS1 expression by macrophages could affect antigen-specific T cell responses. Similar frequencies of PPD-stimulated IFN-γ-secreting CD4^{+} T cells in spleens and lungs from *M. tuberculosis*-infected *LysM-cre SOCS1*$^{fl/fl}$ and *SOCS1*$^{fl/fl}$ controls were found, whereas cells from uninfected mice showed no PPD responses (supplemental Fig. S4*C*).

Lungs from *RAG1*$^{-/-}$ mice at 24 days after *M. tuberculosis* infection showed small amounts of granulomatous lesions that, altogether, made up a minor percentage of the lung area. The lungs from these mice remained otherwise free of inflammatory lesions. In contrast, *RAG1*$^{-/-}$/*SOCS1*$^{-/-}$ mice showed a spectacular pathology, where most of the lung parenchyma was consolidated, showing an atypical proliferative interstitial pneumonitis formed by hyperplastic type II pneumocytes, macrophages, and neutrophils. Large numbers of neutrophils were observed within large areas of necrosis as well as around the blood vessels (Fig. 7, *B–D*).

Similarly, lungs from *IFN-γ*$^{-/-}$/*SOCS1*$^{-/-}$ mice 3 weeks after *M. tuberculosis* infection showed interstitial pneumonia with thickening of the alveolar septa, leaving less area of lung parenchyma free of lesions than in *IFN-γ*$^{-/-}$ controls (Fig. 7, *E–G*). Lungs from *IFN-γ*$^{-/-}$ and IFN-γ$^{-/-}$/*SOCS1*$^{-/-}$ had, in contrast to *RAG1*$^{-/-}$ or *RAG1*$^{-/-}$/*SOCS1*$^{-/-}$ mice, well limited granulomas formed by aggregates of macrophages or epithelioid cells with marked infiltration of neutrophils and variable numbers of lymphocytes. The granulomas were generally rounder, smaller, and better defined in *IFN-γ*$^{-/-}$ than in *IFN-γ*$^{-/-}$/*SOCS1*$^{-/-}$ mice. Thus, the total area of lung parenchyma occupied by granulomas was larger and lymphocytes within the granulomas were more abundant in *IFN-γ*$^{-/-}$/*SOCS1*$^{-/-}$ than in *IFN-γ*$^{-/-}$ mice (Fig. 7, *E–G*). As expected, *M. tuberculosis*-infected *IFN-γ*$^{-/-}$ and *IFN-γ*$^{-/-}$/*SOCS1*$^{-/-}$ lungs showed no increased *iNOS*, *CXCL9*, or *CXCL10* mRNA levels compared with uninfected controls, whereas transcript levels were increased in lungs from WT-infected mice (supplemental Fig. S4, *F–H*).

Importantly, lungs from *LysM-cre SOCS1*$^{fl/fl}$ showed similar histopathological features as SOCS1$^{fl/fl}$ mice 3 and 6 weeks after *M. tuberculosis* infection, with only the exception of a slightly increased interstitial inflammation 6 weeks after infection (Fig. 7, *I* and *J*, and supplemental Fig. S4, *I* and *J*). Altogether, SOCS1 expression by macrophages or neutrophils thus seems to hamper control of *M. tuberculosis in vivo* early after infection, whereas SOCS1 expression in non-macrophage cells can protect mice from infection-induced damaging inflammation.

DISCUSSION

We here report that infection with virulent or avirulent mycobacteria induces SOCS1 expression in mouse and human macrophages and dendritic cells *in vitro*, and *in vivo* in a murine model. SOCS1 expression in macrophages required phagocytosis of mycobacteria and was largely mediated by MyD88/TLR2 and NOD2 receptors. The ensuing NF-κB pathway downstream of both MyD88 and NOD2 receptor signaling was also required. Thus, TLR and non-TLR signals cooperate in *SOCS1* mRNA expression by mycobacteria-infected BMM. IFN-α/β signaling was also required for mycobacterial induced SOCS1 expression by BMM. SOCS1 has been shown to hamper growth control of intracellular infections by *Chlamydia* and *Leishmania* (12, 33), explained by the essential role of SOCS1 in the control of macrophage activation by regulating TLR signaling (24, 46).

We here showed by using knock-out, conditional knockdown, and SOCS1 mimetic peptides that SOCS1 also inhibited growth control of *M. tuberculosis* and BCG by macrophages. Surprisingly, SOCS1 inhibition of BCG and *M. tuberculosis* growth control in BMM was mediated by its ability to obstruct IFN-γ secretion from these cells rather than by an inhibition of responses to IFN-γ. This SOCS1-mediated inhibition of bacterial control was not mediated by a diminished release of IL-12. Instead, SOCS1-deficient BMM proved to be hyperresponsive to IL-12. Neutralization of IL-12 hindered IFN-γ expression in infected *SOCS1*$^{-/-}$ BMM, suggesting a novel mechanism of mycobacterial inhibition of phagocyte activation. The increased response to IL-12 of *SOCS1*$^{-/-}$ BMM was associated with increased levels of *IL-12Rβ1* mRNA before as well as after infection with *M. tuberculosis*. IL-12Rβ1 is expressed on a variety of immune cells, including T, NK, macrophages, and dendritic cells (47–49); is up-regulated by IL-12 and IFN-γ signaling (49); and serves in humans to enhance immunity to mycobacterial pathogens (50, 51). However, increased responses to IL-12 by BMM were not due to an SOCS1-mediated defect in IL-12Rβ1 expression because increased expression of IL-12 is IFN-γ-dependent. In concurrence with our results, *SOCS1*-deficient T cells and dendritic cells showed higher IFN-γ secretion in response to IL-12 (16, 52, 53). JAK2 and TYK2 kinases that are associated with IL-12R will activate and phosphorylate STAT4 upon binding of IL-12. SOCS1 has been shown to bind to JAK2 and inhibit both the kinase activity and the subsequent IL-12 signaling (54).

The expression microarray analysis showed, in agreement with previous reports, that a significant segment of the macrophage transcriptome is altered after infection with *M. tuberculosis* (55, 56). Unexpectedly, the majority of infection-regulated genes overlapped with those differentially regulated by SOCS1, strongly suggesting a major role of SOCS1 in the control of metabolic activity of macrophages during the infection with *M. tuberculosis*. Equally surprising was the finding that the majority of these differentially expressed genes were down-regulated in infected compared with uninfected BMM. The expression of most of these genes was further down-regulated

FIGURE 7. **SOCS1 deficiency in non-macrophage cells mediates increased severity of pulmonary inflammation.** Shown are bacterial load in lungs and spleens of mice (*A*) and histopathological scoring of hematoxylin-eosin-stained paraffin lung sections (*B–D*) from *RAG1*$^{-/-}$/*SOCS1*$^{-/-}$ and *RAG1*$^{-/-}$ mice measured 24 days after aerosol infection with *M. tuberculosis*. *E–G*, pulmonary histopathology of lung sections from *IFN-γ*$^{-/-}$/*SOCS1*$^{-/-}$ and *IFN-γ*$^{-/-}$ mice sacrificed 4 weeks after infection. *, differences with the control group are significant ($p < 0.05$, Mann-Whitney *U* test). Bacterial load in lungs and spleens (*H*) and histopathological scoring of hematoxylin-eosin-stained paraffin lung sections from *LysM-cre SOCS1*$^{fl/fl}$ and *SOCS1*$^{fl/fl}$ (*I* and *J*) mice measured 24 days after infection with *M. tuberculosis*. *Error bars*, S.E.

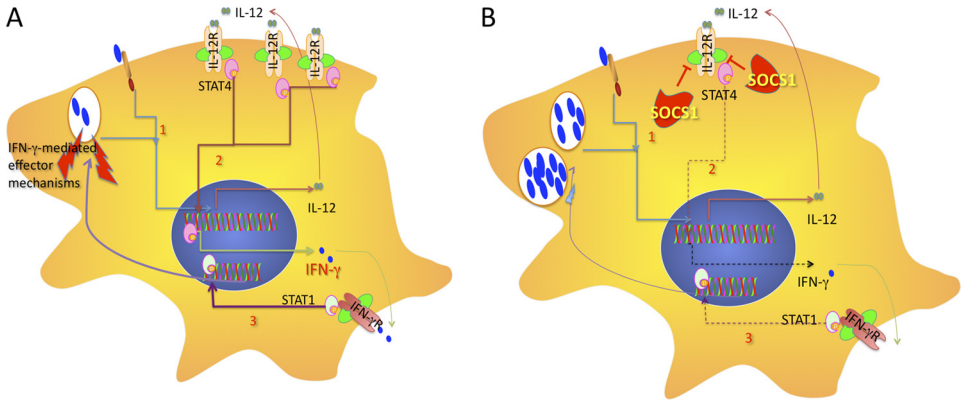

FIGURE 8. **Macrophage responses during *M. tuberculosis* infection in the absence (*A*) or presence (*B*) of SOCS1.** Infection of macrophages with *M. tuberculosis* induces SOCS1 and secretion of IL-12 in an TLR2/MyD88- and NOD2-mediated manner. SOCS1 probably hampers STAT4 activation and reduces IFN-γ secretion in response to *M. tuberculosis*-stimulated IL-12. Decreased IFN-γ levels account for diminished levels of activated STAT1 and IFN-regulated effector molecules in the presence of SOCS1. IFN-γ-dependent IL-12Rβ1 expression is also decreased in the presence of SOCS1. As a consequence, higher intracellular mycobacterial levels are observed. Of importance, SOCS1 does not hinder responses to IFN-γ. The secretion of IFN-α/β is also inhibited.

in *M. tuberculosis*-infected *SOCS1*$^{-/-}$ BMM compared with WT controls. On the contrary, the majority of genes involved in defense or immune responses (data not shown) and almost all IFN-regulated immune genes as well as IFN-β and IFN-γ themselves showed higher levels in the *SOCS1*$^{-/-}$-infected cells (supplemental Table SI). Altogether, our data suggest that SOCS1 attenuates both the negative and the positive regulation of the majority of the genes changing their expression after infection of macrophages with *M. tuberculosis*.

Of importance, we demonstrated that SOCS1 expression by macrophages impaired *M. tuberculosis* clearance and IFN-γ and iNOS expression in mice, when measured 7 days after infection. At this early stage of infection, when increased secretion of IFN-γ is not detected in lungs from infected WT mice, a higher level of IFN-γ secreted by SOCS1-deficient macrophages is sufficient to impair bacterial growth *in vivo*.

Instead, the inability of SOCS1 to hamper bacterial control at later time points, when IFN-γ secretion by T cells is prominent, may thus be explained by the above mentioned capacity of infected, SOCS1-expressing macrophages to respond to IFN-γ. In line with this, similar levels of IFN-γ and IFN-γ-regulated gene transcripts were present in lungs from *SOCS1*$^{-/-}$ mice 3 weeks after infection. Relevant to our observation, SOCS1 expression in blood is increased in pulmonary tuberculosis patients that in parallel express an IFN-regulated gene signature (57).

We also observed an overwhelming infection-induced pulmonary inflammation in *RAG1*$^{-/-}$/*SOCS1*$^{-/-}$ and *IFN-γ*$^{-/-}$/*SOCS1*$^{-/-}$ mice. Because *LysM-cre SOCS1*$^{fl/fl}$ mice, in contrast, showed no increased pathology, we conclude that SOCS1-expressing non-macrophage cells are the main controllers of detrimental inflammation. *SOCS1* silencing in macrophages or dendritic cells has been shown to potentiate anti-tumor immune responses (34), whereas SOCS1 deficiency in whole organs except for T and B cells enhances inflammation-mediated colon tumor development (58).

In summary, we propose a model in which *M. tuberculosis* actively promotes SOCS1 expression by macrophages to counteract effective mycobacterial control at early time points after infection *in vivo*, before initiation of IFN-γ secretion by NK or T cells. SOCS1 facilitates mycobacterial growth by hampering macrophage IFN-γ secretion in response to infection-induced IL-12 (Fig. 8). At later time points after infection, despite SOCS1 expression, macrophages respond to IFN-γ secreted by T cells or NK cells and will not counteract bacterial control to any further extent. Instead, SOCS1 in non-macrophage cells protects mice from severe inflammation.

The mechanisms behind the anti-inflammatory properties of SOCS1 during *M. tuberculosis* remain to be studied. We suggest that the efficient stimulation of SOCS1 expression reflects an evolutionary adaptation that may be associated with the ability of *M. tuberculosis* to establish a chronic infection.

Acknowledgments—We thank Dr. Fredric Carlsson for comments, Dr. Andzej Pawlowski for help and advice with M. tuberculosis infections, and Berit Olsson and Helene Braxenholm for excellent technical assistance (all from Karolinska Institutet); Dr. Robert Geffers (HZI, Braunschweig) for the analysis of the microarray data; Ewa Westergren (Swedish University of Agricultural Sciences) for the preparation of histological slides; Dr. H. Johnson (University of Florida) for the gift of SOCS1 mimetic peptides; and Dr. T. Naka and T. Kishimoto (Osaka University, Japan) for kindly providing SOCS1$^{+/-}$ *mice.*

REFERENCES

1. World Health Organization (2006) *Global Tuberculosis Control: Surveillance, Planning, Financing*, p. 1, World Health Organization, Geneva, Switzerland
2. Nathan, C. F., Murray, H. W., Wiebe, M. E., and Rubin, B. Y. (1983) *J. Exp. Med.* **158,** 670–689
3. Cooper, A. M., Dalton, D. K., Stewart, T. A., Griffin, J. P., Russell, D. G., and Orme, I. M. (1993) *J. Exp. Med.* **178,** 2243–2247
4. Flynn, J. L., Chan, J., Triebold, K. J., Dalton, D. K., Stewart, T. A., and Bloom, B. R. (1993) *J. Exp. Med.* **178,** 2249–2254
5. Casanova, J. L., and Abel, L. (2002) *Annu. Rev. Immunol.* **20,** 581–620
6. Hmama, Z., Gabathuler, R., Jefferies, W. A., de Jong, G., and Reiner, N. E. (1998) *J. Immunol.* **161,** 4882–4893
7. Hussain, S., Zwilling, B. S., and Lafuse, W. P. (1999) *J. Immunol.* **163,** 2041–2048
8. Wojciechowski, W., DeSanctis, J., Skamene, E., and Radzioch, D. (1999) *J. Immunol.* **163,** 2688–2696
9. Yoshimura, A., Naka, T., and Kubo, M. (2007) *Nat. Rev. Immunol.* **7,** 454–465

10. Kile, B. T., and Alexander, W. S. (2001) *Cell Mol. Life Sci.* **58,** 1627–1635
11. Sakamoto, H., Yasukawa, H., Masuhara, M., Tanimura, S., Sasaki, A., Yuge, K., Ohtsubo, M., Ohtsuka, A., Fujita, T., Ohta, T., Furukawa, Y., Iwase, S., Yamada, H., and Yoshimura, A. (1998) *Blood* **92,** 1668–1676
12. Alexander, W. S., Starr, R., Fenner, J. E., Scott, C. L., Handman, E., Sprigg, N. S., Corbin, J. E., Cornish, A. L., Darwiche, R., Owczarek, C. M., Kay, T. W., Nicola, N. A., Hertzog, P. J., Metcalf, D., and Hilton, D. J. (1999) *Cell* **98,** 597–608
13. Marine, J. C., Topham, D. J., McKay, C., Wang, D., Parganas, E., Stravopodis, D., Yoshimura, A., and Ihle, J. N. (1999) *Cell* **98,** 609–616
14. Naka, T., Tsutsui, H., Fujimoto, M., Kawazoe, Y., Kohzaki, H., Morita, Y., Nakagawa, R., Narazaki, M., Adachi, K., Yoshimoto, T., Nakanishi, K., and Kishimoto, T. (2001) *Immunity* **14,** 535–545
15. Chong, M. M., Cornish, A. L., Darwiche, R., Stanley, E. G., Purton, J. F., Godfrey, D. I., Hilton, D. J., Starr, R., Alexander, W. S., and Kay, T. W. (2003) *Immunity* **18,** 475–487
16. Chong, M. M., Metcalf, D., Jamieson, E., Alexander, W. S., and Kay, T. W. (2005) *Blood* **106,** 1668–1675
17. Fenner, J. E., Starr, R., Cornish, A. L., Zhang, J. G., Metcalf, D., Schreiber, R. D., Sheehan, K., Hilton, D. J., Alexander, W. S., and Hertzog, P. J. (2006) *Nat. Immunol.* **7,** 33–39
18. Eyles, J. L., Metcalf, D., Grusby, M. J., Hilton, D. J., and Starr, R. (2002) *J. Biol. Chem.* **277,** 43735–43740
19. Dickensheets, H., Vazquez, N., Sheikh, F., Gingras, S., Murray, P. J., Ryan, J. J., and Donnelly, R. P. (2007) *Genes Immun.* **8,** 21–27
20. Cornish, A. L., Chong, M. M., Davey, G. M., Darwiche, R., Nicola, N. A., Hilton, D. J., Kay, T. W., Starr, R., and Alexander, W. S. (2003) *J. Biol. Chem.* **278,** 22755–22761
21. Vázquez, N., Greenwell-Wild, T., Rekka, S., Orenstein, J. M., and Wahl, S. M. (2006) *J. Leukoc. Biol.* **80,** 1136–1144
22. Imai, K., Kurita-Ochiai, T., and Ochiai, K. (2003) *FEMS. Immunol. Med. Microbiol.* **39,** 173–180
23. Srivastava, V., Manchanda, M., Gupta, S., Singla, R., Behera, D., Das, G., and Natarajan, K. (2009) *J. Biol. Chem.* **284,** 25532–25541
24. Nakagawa, R., Naka, T., Tsutsui, H., Fujimoto, M., Kimura, A., Abe, T., Seki, E., Sato, S., Takeuchi, O., Takeda, K., Akira, S., Yamanishi, K., Kawase, I., Nakanishi, K., and Kishimoto, T. (2002) *Immunity* **17,** 677–687
25. Kawai, T., Adachi, O., Ogawa, T., Takeda, K., and Akira, S. (1999) *Immunity* **11,** 115–122
26. Sato, M., Suemori, H., Hata, N., Asagiri, M., Ogasawara, K., Nakao, K., Nakaya, T., Katsuki, M., Noguchi, S., Tanaka, N., and Taniguchi, T. (2000) *Immunity* **13,** 539–548
27. Takeuchi, O., Hoshino, K., Kawai, T., Sanjo, H., Takada, H., Ogawa, T., Takeda, K., and Akira, S. (1999) *Immunity* **11,** 443–451
28. Hoshino, K., Takeuchi, O., Kawai, T., Sanjo, H., Ogawa, T., Takeda, Y., Takeda, K., and Akira, S. (1999) *J. Immunol.* **162,** 3749–3752
29. Kobayashi, K. S., Chamaillard, M., Ogura, Y., Henegariu, O., Inohara, N., Nuñez, G., and Flavell, R. A. (2005) *Science* **307,** 731–734
30. Huang, S., Hendriks, W., Althage, A., Hemmi, S., Bluethmann, H., Kamijo, R., Vilcek, J., Zinkernagel, R. M., and Aguet, M. (1993) *Science* **259,** 1742–1745
31. Müller, U., Steinhoff, U., Reis, L. F., Hemmi, S., Pavlovic, J., Zinkernagel, R. M., and Aguet, M. (1994) *Science* **264,** 1918–1921
32. Mombaerts, P., Iacomini, J., Johnson, R. S., Herrup, K., Tonegawa, S., and Papaioannou, V. E. (1992) *Cell* **68,** 869–877
33. Yang, T., Stark, P., Janik, K., Wigzell, H., and Rottenberg, M. E. (2008) *J. Immunol.* **180,** 4040–4049
34. Hashimoto, M., Ayada, T., Kinjyo, I., Hiwatashi, K., Yoshida, H., Okada, Y., Kobayashi, T., and Yoshimura, A. (2009) *Cancer Sci.* **100,** 730–736
35. Clausen, B. E., Burkhardt, C., Reith, W., Renkawitz, R., and Förster, I. (1999) *Transgenic Res.* **8,** 265–277
36. Rothfuchs, A. G., Gigliotti, D., Palmblad, K., Andersson, U., Wigzell, H., and Rottenberg, M. E. (2001) *J. Immunol.* **167,** 6453–6461
37. Davies, J. Q., and Gordon, S. (2005) *Methods Mol. Biol.* **290,** 105–116
38. Chackerian, A. A., Alt, J. M., Perera, T. V., Dascher, C. C., and Behar, S. M. (2002) *Infect. Immun.* **70,** 4501–4509
39. Rothfuchs, A. G., Trumstedt, C., Mattei, F., Schiavoni, G., Hidmark, A., Wigzell, H., and Rottenberg, M. E. (2006) *J. Immunol.* **176,** 6982–6990
40. Underhill, D. M., Ozinsky, A., Smith, K. D., and Aderem, A. (1999) *Proc. Natl. Acad. Sci. U.S.A.* **96,** 14459–14463
41. Thoma-Uszynski, S., Stenger, S., Takeuchi, O., Ochoa, M. T., Engele, M., Sieling, P. A., Barnes, P. F., Rollinghoff, M., Bolcskei, P. L., Wagner, M., Akira, S., Norgard, M. V., Belisle, J. T., Godowski, P. J., Bloom, B. R., and Modlin, R. L. (2001) *Science* **291,** 1544–1547
42. Abel, B., Thieblemont, N., Quesniaux, V. J., Brown, N., Mpagi, J., Miyake, K., Bihl, F., and Ryffel, B. (2002) *J. Immunol.* **169,** 3155–3162
43. Gandotra, S., Jang, S., Murray, P. J., Salgame, P., and Ehrt, S. (2007) *Infect. Immun.* **75,** 5127–5134
44. Flowers, L. O., Johnson, H. M., Mujtaba, M. G., Ellis, M. R., Haider, S. M., and Subramaniam, P. S. (2004) *J. Immunol.* **172,** 7510–7518
45. Ahmed, C. M., Dabelic, R., Waiboci, L. W., Jager, L. D., Heron, L. L., and Johnson, H. M. (2009) *J. Virol.* **83,** 1402–1415
46. Kinjyo, I., Hanada, T., Inagaki-Ohara, K., Mori, H., Aki, D., Ohishi, M., Yoshida, H., Kubo, M., and Yoshimura, A. (2002) *Immunity* **17,** 583–591
47. Puddu, P., Fantuzzi, L., Borghi, P., Varano, B., Rainaldi, G., Guillemard, E., Malorni, W., Nicaise, P., Wolf, S. F., Belardelli, F., and Gessani, S. (1997) *J. Immunol.* **159,** 3490–3497
48. Munder, M., Mallo, M., Eichmann, K., and Modolell, M. (1998) *J. Exp. Med.* **187,** 2103–2108
49. Musikacharoen, T., Oguma, A., Yoshikai, Y., Chiba, N., Masuda, A., and Matsuguchi, T. (2005) *Blood* **105,** 711–720
50. Altare, F., Durandy, A., Lammas, D., Emile, J. F., Lamhamedi, S., Le Deist, F., Drysdale, P., Jouanguy, E., Döffinger, R., Bernaudin, F., Jeppsson, O., Gollob, J. A., Meinl, E., Segal, A. W., Fischer, A., Kumararatne, D., and Casanova, J. L. (1998) *Science* **280,** 1432–1435
51. de Jong, R., Altare, F., Haagen, I. A., Elferink, D. G., Boer, T., van Breda Vriesman, P. J., Kabel, P. J., Draaisma, J. M., van Dissel, J. T., Kroon, F. P., Casanova, J. L., and Ottenhoff, T. H. (1998) *Science* **280,** 1435–1438
52. Evel-Kabler, K., Song, X. T., Aldrich, M., Huang, X. F., and Chen, S. Y. (2006) *J. Clin. Invest.* **116,** 90–100
53. Hanada, T., Tanaka, K., Matsumura, Y., Yamauchi, M., Nishinakamura, H., Aburatani, H., Mashima, R., Kubo, M., Kobayashi, T., and Yoshimura, A. (2005) *J. Immunol.* **174,** 4325–4332
54. Davey, G. M., Heath, W. R., and Starr, R. (2006) *Tissue Antigens* **67,** 1–9
55. Ehrt, S., Schnappinger, D., Bekiranov, S., Drenkow, J., Shi, S., Gingeras, T. R., Gaasterland, T., Schoolnik, G., and Nathan, C. (2001) *J. Exp. Med.* **194,** 1123–1140
56. Shi, S., Nathan, C., Schnappinger, D., Drenkow, J., Fuortes, M., Block, E., Ding, A., Gingeras, T. R., Schoolnik, G., Akira, S., Takeda, K., and Ehrt, S. (2003) *J. Exp. Med.* **198,** 987–997
57. Berry, M. P., Graham, C. M., McNab, F. W., Xu, Z., Bloch, S. A., Oni, T., Wilkinson, K. A., Banchereau, R., Skinner, J., Wilkinson, R. J., Quinn, C., Blankenship, D., Dhawan, R., Cush, J. J., Mejias, A., Ramilo, O., Kon, O. M., Pascual, V., Banchereau, J., Chaussabel, D., and O'Garra, A. (2010) *Nature* **466,** 973–977
58. Hanada, T., Kobayashi, T., Chinen, T., Saeki, K., Takaki, H., Koga, K., Minoda, Y., Sanada, T., Yoshioka, T., Mimata, H., Kato, S., and Yoshimura, A. (2006) *J. Exp. Med.* **203,** 1391–1397